Design of Large Finite Arrays Using Simulations or Measurements of Small Arrays

Ahmed A. Kishk
Department of Electrical and Computer Engineering
Concordia University, Montreal, CANADA
(Email: kishk@encs.concordia.ca)

***Abstract*—A simple and efficient procedure is proposed to predict the performance of large finite arrays from the measurements of a small array of similar lattice. The procedure depends on the knowledge of the mutual admittance matrix of the small array from which the mutual admittance matrix of the larger array is constructed by ignoring the mutual coupling between the elements that are external to the domain of the small array. Once the admittance matrix has been constructed for the large array, active input impedances of the array elements under different scenarios can be predicted easily. Also, from the active voltage terminal of the elements, an array factor including the mutual coupling can be computed to predict the radiation patterns as well as the array gain. Here, an air microstrip patch antenna excited by a hook-shaped probe is considered as an array element. The results obtained using the present method is verified by the full-wave numerical analysis of the large array. The results obtained serve to verify the concept.**

***Index Terms*—Finite Array, Large Array, Microstrip Antenna, Phased Array.**

I. INTRODUCTION

Predicting radiation characteristics of a large array can be an easy task if the mutual coupling between the elements can be ignored. Pattern multiplication method of the array factor, and the single element radiation pattern of an isolated element or in the array environment, could be sufficient to predict the array radiation characteristics. However, determining the effective input impedances at the antenna terminals (input impedance while all the elements are active), is not a simple task and it is time-consuming if one needs to measure them. Since the demand for phased arrays, which provide electronic scanning capabilities has increased for satellite, military and vehicular communications increased, needs for accurate analysis and measurements becomes necessary. However, accurate design requires a full-wave analysis of the array. With the advancements in the computation methods, array analysis and design of large array have now become possible. However, such analyses can be highly computer-intensive and costly, since they require the use of expensive commercial codes [1, 2]. In fact, for very large arrays, such analysis may not even be feasible, unless we resort to parallel computing or use special numerical techniques. Although numerous design techniques can be found in the literature [3]-[22], these techniques are limited in their applicability to certain types of arrays with specific types of elements. Furthermore, it may be necessary to tailor the algorithm to the type of elements and, hence, modify it if element-type is changed. In some cases the formulation of the problem changes as the element type changes. The need for an efficient method to analyze large array is growing.

In phased arrays, the mutual coupling has a pronounced effect on the performance as the scan range is increased. Mutual coupling changes the performance of a single element in the sense that the coupling between different elements is likely to affect the resonance frequency and the radiated power of each element. To account for this, there has been a considerable interest in developing techniques for including the mutual coupling effects into the design techniques for phased arrays; however, such techniques are both complex and computer intensive. To reduce the design costs and risks, and to improve the performance of the arrays simulations, the design method should be computationally efficient, include effects of mutual coupling, and should be able to determine the array performance for the entire scan range. Furthermore, it should be able to predict the matching performance within the scan range and the effect of failing elements in the array. Therefore, in order to design these arrays and their feeding network to accommodate the wide-angle scanning capabilities and to account for their effect on the matching of the array elements, a computationally efficient method needs to be developed. Usually, for a very large finite array, the analysis of single element in an infinite array environment is performed numerically, and the analysis of the large arrays is then extrapolated from this analysis. However, the elements near the edge perform differently from the rest of the array elements, and the analysis may have to be repeated, for each scan direction. Simulations based on the generally employed infinite-array approach and simulations based on the periodic version of the finite-element method do not satisfy these criteria. Simulations using the infinite array environment do not describe the edge effects, while simulations of large finite arrays are computationally too expensive. Furthermore, neither of these simulations provide direct insight into the physics relevant to the design. To overcome these disadvantages, simple simulation tools for large arrays are desired.

In this paper, the technique described in [23, 24] is used to develop a procedure for the design of planar antenna arrays. The design expressions are used in a rather general form to analyze arrays of similar elements. This technique has been presented in [25] and implemented in a near-field focusing array [26]. Here, we propose a technique which leverages the advantages of numerical techniques and the availability of efficient commercial codes, such as WIPL-D [27], to analyze a small array, and use the computed parameters to predict and design a larger array, which has a similar lattice.

II. Analysis of Planar Array

For an array of N elements, the antenna element is considered as a load in series with internal resistance of the source as shown in Fig. 1. The mutual coupling between the elements changes the elements terminal voltages as shown in Fig. 2. It is important to derive a relationship between the effective voltage across the input terminals of the antenna and the applied voltage (source voltage). If I_i is the current supplied by the source voltage V_i to the i-th radiating element, the effective voltage V_{ai} at the input terminals of that element is determined through the relation [23]

$$I_i = (V_i - V_{ai}) / R_i \tag{1}$$

where R_i is the internal resistance of the source and i=1,2...N..

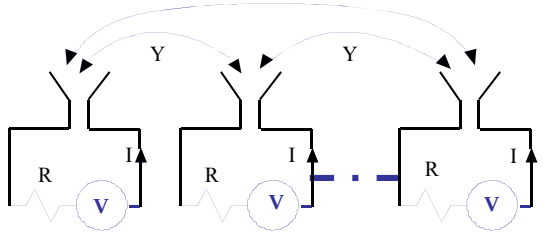

Fig. 1 Equivalent circuit of an antenna array

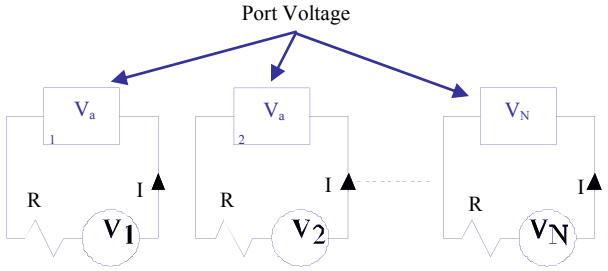

Fig. 2 Equivalent circuit for the effective voltages of the antenna array.

Fig. 2 indicates that I_i is linearly related to the effective voltages across input terminals.

$$I_i = \sum_{j=1}^{N} Y_{ij} V_{aj} \tag{2}$$

where Y_{ii} is the self-admittance of the i-th element and Y_{ij} is the mutual admittance seen by the feed between the i-th and j-th radiating elements. From (1) and (2), the effective voltage can be expressed as

$$\sum_{j=1}^{N} (Y_{ij} R_i + \delta_{ij}) V_{aj} = V_i \tag{3}$$

where δ_{ij} = 1 for $i = j$ and zero for $i \neq j$. This equation can be expressed in a matrix form as

$$[V_a] = [A_{ij}] [V] \tag{4}$$

where

$$[A_{ij}] = [Y_{ij} R_i + \delta_{ij}]^{-1} \tag{5}$$

The effective voltage across the i-th element can be derived as

$$V_{ai} = \sum_{j=1}^{N} A_{ij} V_j \tag{6}$$

The effective voltage at the input terminals of each element can be obtained from the known source distribution. If the mutual coupling effects are not included, then the applied voltage V_i appears directly across the input terminals of the patch.

Effective Input Impedance: The effect of mutual coupling on the input impedance of each element in an array can be expressed as

$$Z_i^e = V_{ia} / I_i, \tag{7}$$

which in turn, can be rewritten as

$$Z_i^e = \sum_{j=1}^{N} A_{ij} V_j / \sum_{j=1}^{N} \sum_{k=1}^{N} Y_{ik} A_{kj} V_j \tag{8}$$

Also, using (1) to (4) Z_i^e can be expressed as

$$Z_i^e = R_i \sum_{j=1}^{N} A_{ij} V_j / \sum_{j=1}^{N} (\delta_{ij} - A_{ij}) V_j \tag{9}$$

for $R_i \neq 0$. If the mutual coupling effects are not included, then the input impedance of the element is equal to that of an isolated element. It should be mentioned that the mutual impedance matrix is independent of the excitation sources that are used to control the scanning and the side lobe level. However, the effective impedances strongly depend on the mutual impedance matrix and the excitation of the array. This simple procedure could also be used to study the effect of shorting or open circuiting any antenna port within the array by changing the value of the internal impedance of the source.

Radiation Patterns of a Planar Array: Consider an array of N identical elements in xy-plane. The total field pattern of such an array is the product of the element pattern and the array factor. If (ρ_i, φ_i) are the cylindrical coordinates of the i-th element and E_i is the effective excitation voltage, then the array factor is expressed as

$$F(\theta, \phi) = \sum_{i=1}^{N} V_{ai} e^{j k_o \rho_i \sin\theta \cos(\phi - \phi_i)}. \tag{10}$$

Then, the expressions for total pattern of the array of identical elements are given by

$$\begin{Bmatrix} E_\theta^t \\ E_\phi^t \end{Bmatrix} = \begin{Bmatrix} E_\theta \\ E_\phi \end{Bmatrix} F(\theta, \phi) \tag{11}$$

where E_θ and E_φ are the element patterns, within the array environment. For a phased array, the main beam direction is controlled by the phase of the excitation sources. The phase shift, which should be introduced in the excitation voltage of the i-th element to obtain a main beam in the direction of (θ_0, φ_0), is given by

$$\psi_i = - j k_o \rho_i \sin\theta_o \cos(\phi_o - \phi_i) \tag{12}$$

where ϕ_i is the phase of the excitation voltage V_i. However, the mutual coupling affects the effective voltage magnitude

and phase across the antenna terminals. Therefore, it is possible that the main beam direction and the desired side lobe levels be altered.

Power Gain of an Array Antenna: With the knowledge of effective input impedance and the excitation current, the power delivered to an element can be obtained, where the real part of the power delivered to the *i*-th element, which contributes to the radiation is given by

$$P_i = R_i^e \mid I_i \mid^2 \tag{13}$$

where R_{in}^e is the real part of the effective input impedance Z_i^e. The total input power that contributes to the radiation from the array is obtained as

$$P_T = \sum_{i=1}^{N} P_i = \sum_{i=1}^{N} R_i^e \mid I_i \mid^2 \tag{14}$$

If the radiated power is assumed to be the power radiated by an isotropic source, the power radiated per unit area by the isotropic source is $P_{IR} = P_T/(4\pi r^2)$. The total radiated power density available from the array at a distance r is given as

$$P_{array} = \frac{\mid E_\theta^t \mid^2 + \mid E_\phi^t \mid^2}{120\pi} \tag{15}$$

The gain of the array with respect to an isotropic radiator can be expressed as

$$G(\theta,\ \phi) = 4\pi r^2 \frac{\mid E_\theta^t \mid^2 + \mid E_\phi^t \mid^2}{120\pi P_T} \tag{16}$$

Construction of the Mutual Admittance Matrix for a Large Array:

For simplicity, we will illustrate the procedure, proposed here in, by using a 4-element linear array, with N_s = 4, to construct a linear array of 8 elements, as shown in Fig. 3. The mutual admittance matrix of the small array is of order (4x4) can be presented graphically as shown in Fig. 4a. We simply map the small matrix into the large matrix for the 8-element array, which is an 8x8 matrix, as shown in Fig. 4b. Note that the mutual coupling between elements with distances greater than 3d are ignored and are forced to be zero. The mutual couplings between the elements of the same relative distances and position in the large matrix are retained the same as those in the small matrix. It is also advisable to keep track of the relative positions in the small and large array.

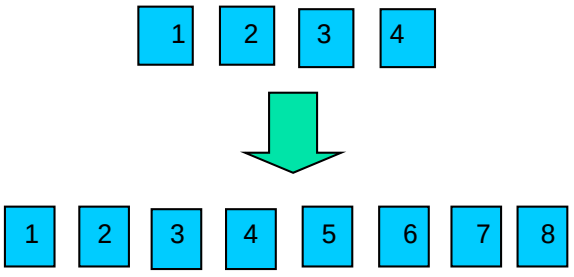

Fig. 3. Linear array of 4 elements that is used to construct a linear array of 8-elements.

1,1	1,2	1,3	1,4
2,1	2,2	2,3	2,4
3,1	3,2	3,3	3,4
4,1	4,2	4,3	4,4

(a) $Y_{i,j}$ (for the 4-element array)

1,1	1,2	1,3	0	0	0	0	0
2,1	2,2	2,3	2,3	0	0	0	0
3,1	3,2	3,3	3,2	2,3	0	0	0
0	2,3	3,2	2,2	2,3	2,3	0	0
0	0	2,3	2,3	3,3	3,2	3,2	0
0	0	0	2,3	3,2	3,3	2,3	2,4
0	0	0	0	2,3	2,3	3,3	3,4
0	0	0	0	0	2,4	3,4	4,4

(b) $Y_{i,j}$ (for the 8-element array)

Fig. 4 Mutual admittance matrix arrangement (a) 4-elemet array and (b) constructed for 8-element array.

For the two-dimensional array, similar logic is used to construct the mutual impedance matrix of the larger array. The large array is represented by M_L elements in the x-direction and N_L in the y-direction. The small array has M_s and N_s elements in the x-and y-directions, respectively. Notice that $M_L \geq M_s$ and $N_L \geq N_s$. If we denote the admittance matrix elements of the large array by the superscript *L* and those for the small array by the superscript *S*, then we have

$$Y_{k\ell}^L = \begin{cases} Y_{ij}^S & i,j = 1,2,...,M_s N_s \\ 0 & otherwise \end{cases} \tag{17}$$

where

$$i_L, j_L = 1,2,...,M_L N_L$$

$$k = M_L(j_L - 1) + i_L' \qquad \ell = N_L(i_L - 1) + j_L'$$

$$i = M_s(j_s - 1) + i_s' \qquad j = N_s(i_s - 1) + j_s'$$

and

$$\mid i_L' - i_L \mid = \mid i_s' - i_s \mid \ \& \ \mid j_L' - j_L \mid = \mid j_s' - j_s \mid$$

III. Numerical Results

To test the procedure described in the last section, an array of rectangular microstrp patches excited by a hook-shaped probe is considered, as shown in Fig. 5. The patch has the dimensions: length 25 mm; width 30 mm; and the height above the ground plane 7.5 mm. The vertical part of the probe that is above the ground plane and just below the patch edge is 6 mm. It is bent horizontally and extended under the patch by 11 mm and then bent vertically toward the ground plane by 2 mm. The ground plane is assumed to be infinite. The input impedance and radiation patterns of this patch are shown in Figs. 6 and 7, respectively. The radiation patterns are obtained at 4.5 GHz. The results are obtained by using the commercial code WIPL-D [25], which is based on the surface integral equations and the Method of Moment (MoM).

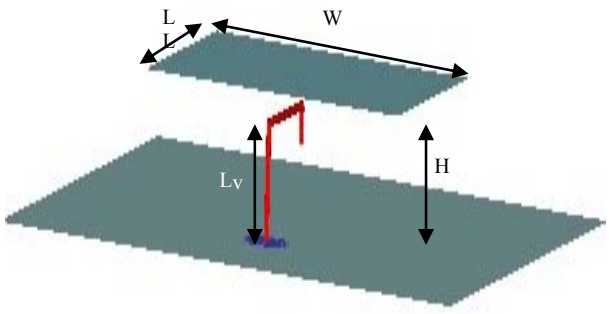

Fig. 5 Geometry of a rectangular patch excited by a Hook-shaped probe.

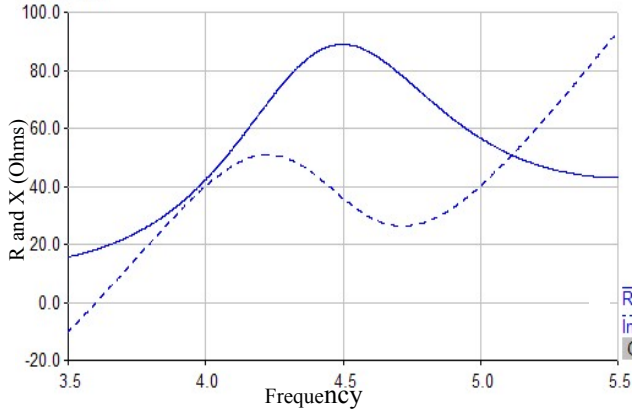

Fig. 6 Input Impedance of the rectangular patch

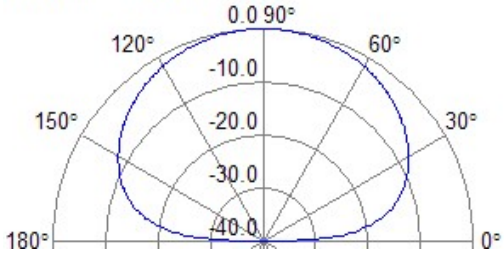

(a) H-plane

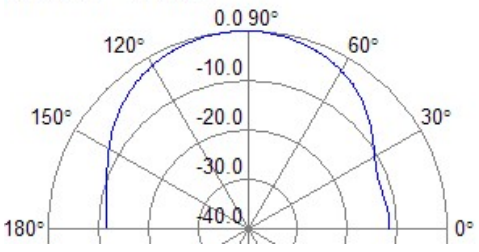

(b) E-plane

Fig. 7 Radiation patterns of the patch at 4.5 GHz.

A 4×4-element array using the patch described above, with center-to-center separation distance of 38 mm between the elements in the x-direction and the y-direction, is analyzed using the WIPL-D code. The code provides the mutual admittance matrix, whose size is on the order 16. This matrix is used to fill the mutual admittance matrix of an 8×8-element array. The effective impedance of the 8×8-element array is computed using the proposed procedure.

Also, this array is analyzed using the WIPL-D code to obtain the effective impedance of the array. Fig. 8 shows a comparison between the effective impedances using the MoM and the one obtained with the present method. Notice that the array was numbered row by row. It can be observed that the edge elements are represented by the effective impedance spikes in both the real and imaginary parts. The radiation patterns of this array, shown in Fig. 9, using array pattern multiplication (APM) compared with the MoM, which include the mutual coupling effects. It should be mentioned that the APM method used the radiation pattern of an isolated element. If the radiation pattern of the element in the array environment is used, an improvement can be obtained particularly at the lower elevation angles. The array gain is computed and found to be 25.86 dB using the APM, as compared to 25.5 dB from MoM.

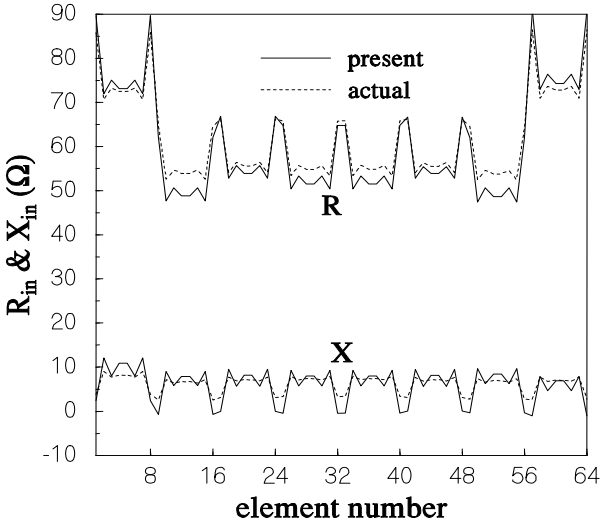

Fig. 8 Effective impedance of 8x8-element array using the 4x4-element array. The dotted curves are the actual impedances from the full wave analysis (WIPL-D).

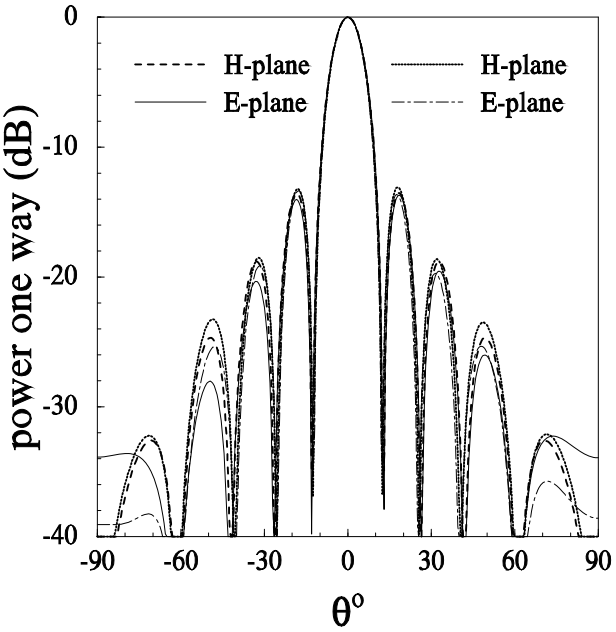

Fig. 9 Radiation patterns of the 8x8-element array. The solid and dashed lines are for the MoM code.

Next, a larger array of 16×16-element array is constructed by using the 4×4-element array. The effective impedances are shown in Fig. 10. The radiation patterns are plotted in Fig. 11. The computed gain is found to be 31.6 dB when using the APM vs. 31.5 dB using the MoM.

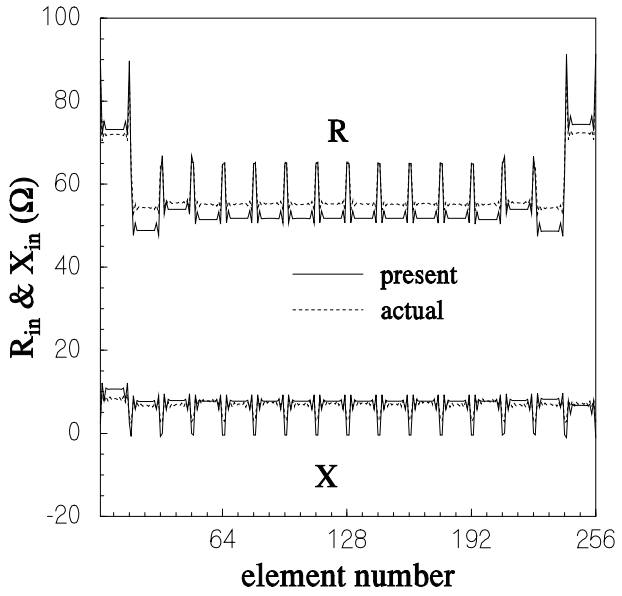

Fig. 10 Effective impedance of 16×16-element array using the 4×4-element array.

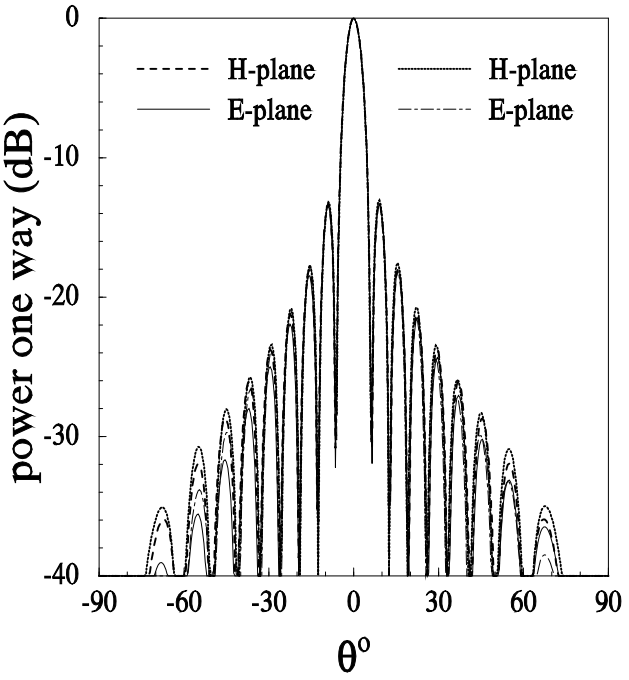

Fig. 11 Radiation patterns of the 16×16-element array using 4×4-element array.

When this array is constructed from an 8x8-element array, the effective input impedance is given in Fig. 12. It can be observed that the impedance prediction becomes more accurate than when the 4×4-element array is used. Fig. 13 shows the radiation patterns. Comparing the radiation patterns in Fig. 11 with those in Fig. 13, we observe better prediction of the far away side lobe levels.

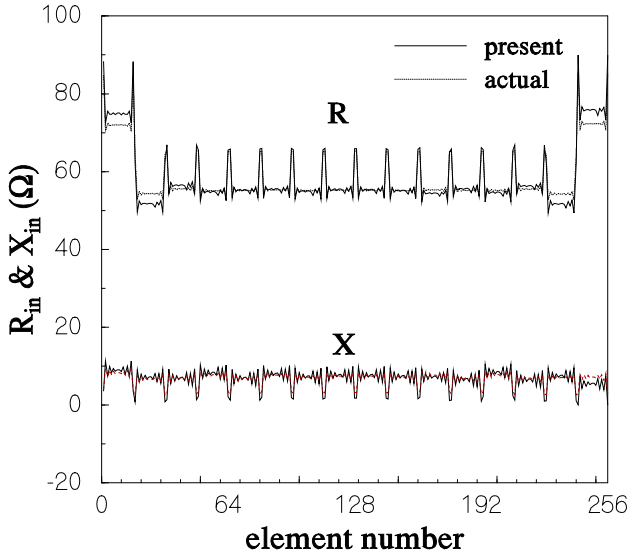

Fig. 12 Effective impedance of 16×16-element array using the 8x8-element array.

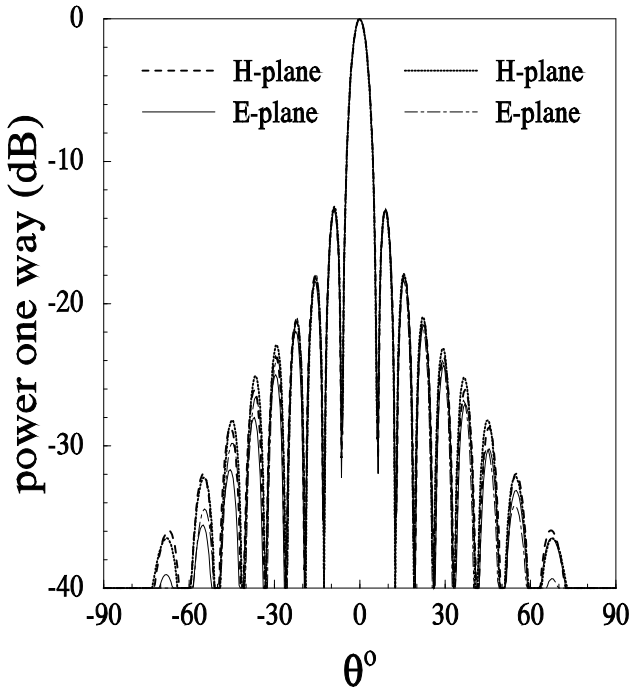

Fig. 13 Radiation patterns of the 16×16-element array using 8X8-element array.

Finally, we move to a 32×32-element array and predict its performance by using a 4x4-element array; an 8×8-element array; and a 16×16-element array. With the current resources we were not able to predict one MoM results for the 32×32-element array. The effective impedance for the 32×32-element array is shown in Fig. 14. From the figure one can see that the 8 × 8-element arrays provide results that are similar to those of the 16×16-element array. Also observe that the 4×4-element array provides a reasonably good prediction for the 32×32-element array and that the results predicted by the 16×16-element array are virtually the same as those for the 32x32-element array (not obtained from full-wave analysis). The 32×32-element array achieves a gain of 37.46 dBi.

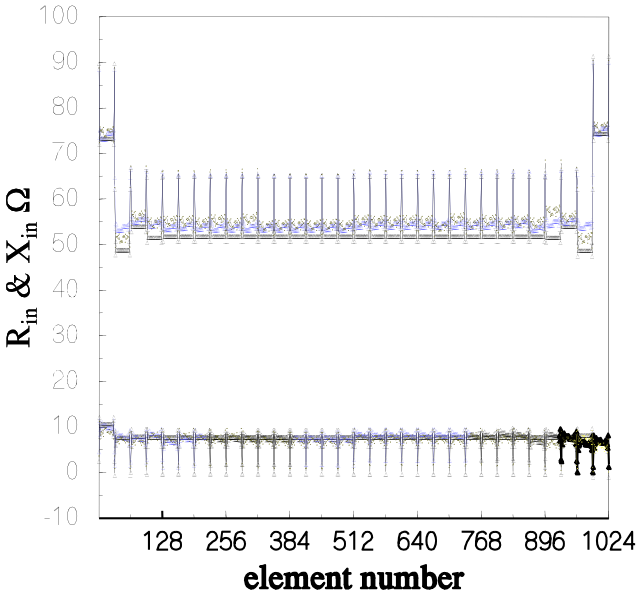

Fig. 14 Effective impedance of 32×32-element array using 4x4 (black), 8×8 (yellow), and 16×16-element array (blue).

Using the same mutual impedance values, we can use different excitations to derive the effective voltages and currents and compute the effective impedances. That is to say using the same A matrix in (4), we can change the vector |V> to obtain different array characteristics. Such information can be used to predict the array performance under different variations of scanning conditions and to know the range of the effective input impedances of the array elements. To illustrate that, let us consider the case of a linear array of 32 elements that is obtained from a 4 element array, whose center-to-center separation is 38 mm. Figs.15-16 show the effective impedance of the array for the H-plane (hook probe plane is normal to the array line) and E-plane (hook probe plane is parallel to the array) arrangements, respectively. The antenna gains were predicted to be 23.7dBi and 23dBi, respectively. When we scan the array off the broadside by 45°, the input effective impedances change as shown in Figs 17 and 18. The radiation patterns predicted by the AFM are in excellent agreement with the actual antenna predicted by the MoM. The gain of the antenna is predicted to be 23.0 and 22.5 dBi, respectively.

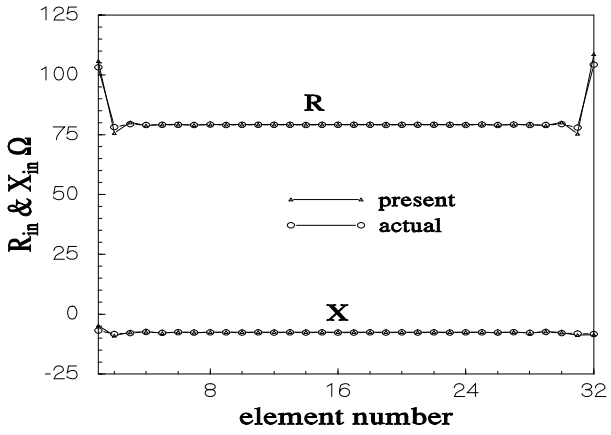

Fig. 15 Effective input impedance of an H-plane 32-element linear array with uniform distribution obtained from 8-element array and compared with the actual array.

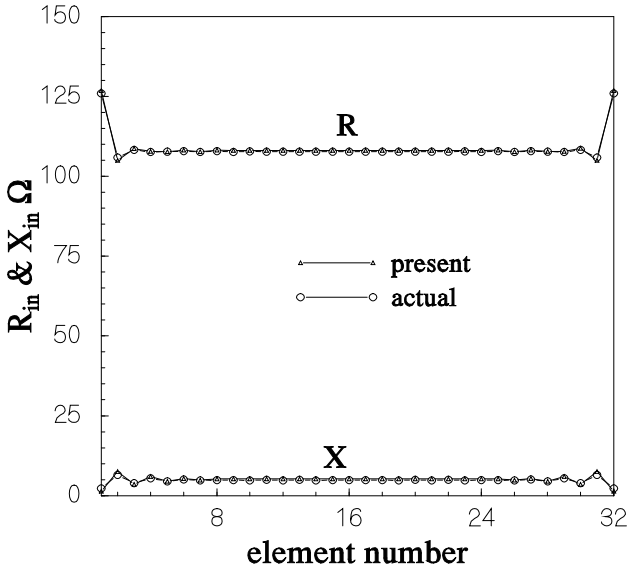

Fig. 16 Effective input impedance of an E-plane linear array of 32 elements with uniform distribution obtained from 8-element array and compared with the actual array.

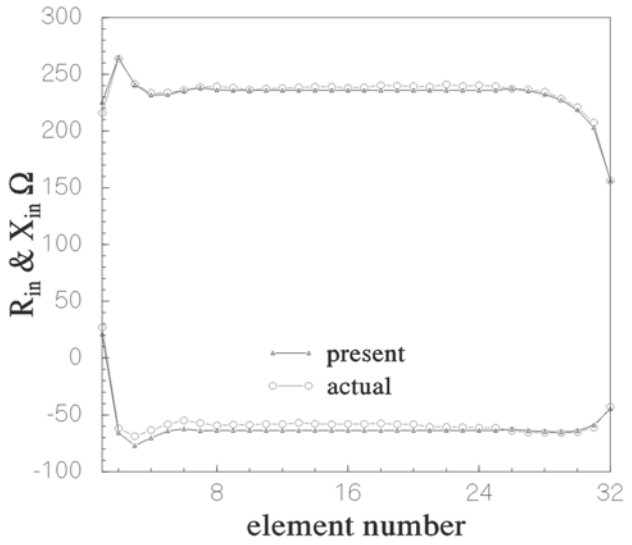

Fig. 17 Effective input impedance of an H-plane linear array of 32 elements with uniform distribution and scanning at 45° and compared with the actual array results.

When we use the Taylor distribution to reduce the sidelobe level to -30 dB, the effective input impedances are obtained as shown in Fig. 19 for the 32-element E-plane array. It can be seen that the impedance level is not that much different from those plotted in Fig.17. The radiation pattern is shown in Fig. 20. When this array, designed to meet the -30 dB sidelobe level requirement is scanned at 45° the effective input impedance is shown in Fig. 21 and the radiation patterns are shown in Fig. 22. A significant change in the effective impedance behaviour is observed and the radiation patterns show a grating lobe at 90°. The mutual coupling pushes the sidelobe above the level of -30dB. It should be mentioned that the radiation patterns for the uniform power distribution case does not show the grating lobe effect since it is below the regular side lobe level.

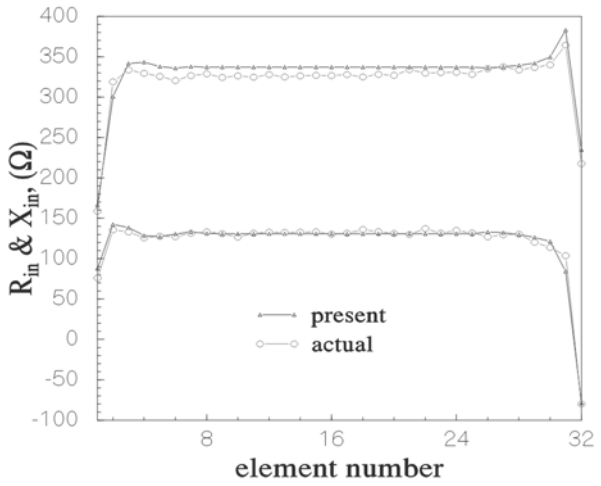

Fig. 18 Effective input impedance of an E-plane linear array of 32 elements with uniform distribution and scanning at 45º and compared with the actual array results.

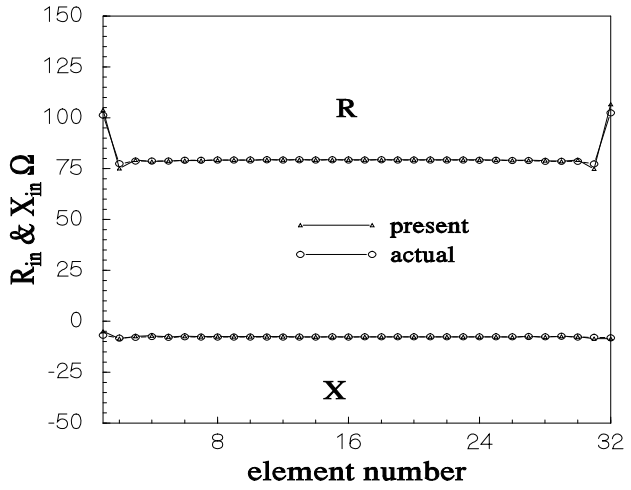

Fig. 19 Effective input impedance of an E-plane linear array of 32 elements with Taylor distribution of -30dB sidelobe level compared with the actual array results.

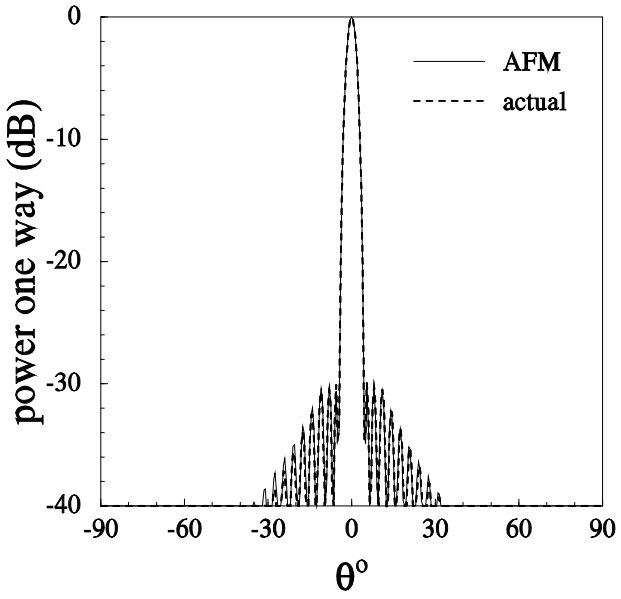

Fig. 20 Radiation patterns of the array in 19.

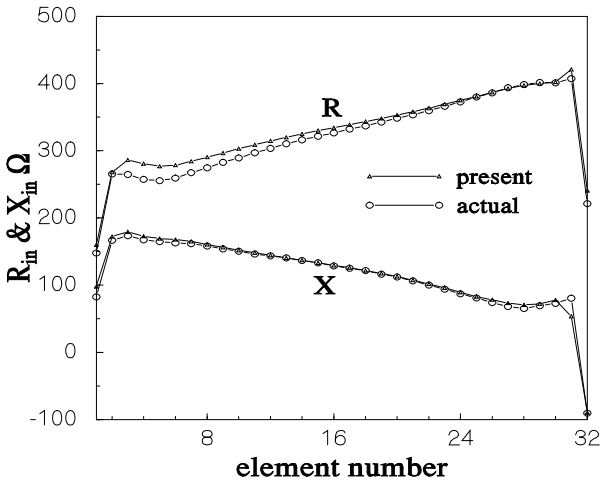

Fig. 21 Effective input impedance of an E-plane linear array of 32 elements with Taylor distribution and -30 DB sidelobe level and scanning at 45o compared with the actual array results.

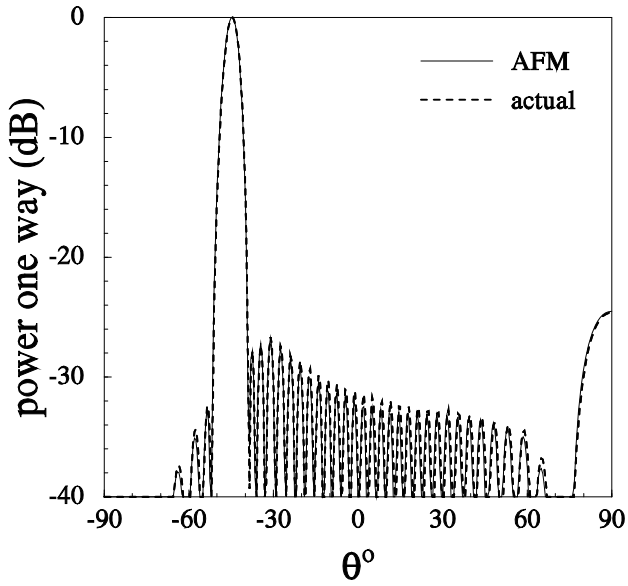

Fig. 22 Radiation patterns of the array in Fig. 21.

The method described above can also be used to study the effect of faulty elements, such as shorted or open circuited elements, or combinations thereof. However, the matrix A has to be constructed using (5) based on the mutual admittance Y of the array and the new internal impedances of the sources.

IV. Conclusions

A simple and efficient procedure has been proposed to predict the performance of large finite arrays from the measurements results of a smaller array. It is necessary to ensure that both arrays have the same lattice arrangements and spacing between the elements. The analyses have been performed numerically; however, experimental study can be used with the small array and the large finite array performance can be predicted based on the measurements of the mutual impedances of the small array. The procedure has

been tested by using an array of air-filled microstrip patch antennas. The results were verified to provide confidence on the proposed procedure. A future analysis will be presented based on the S-parameters of the array and its frequency response, different element types will be investigated and the results will be reported in a future publication.

REFERENCES

[1] D. Parker and D. C. Zimmermann, "Phased arrays – Part I: Theory and Architectures," *IEEE Transactions on Microwave Theory and Techniques*, Vol. 50, pp.678–687, 2002.

[2] D. Parker and D. C. Zimmermann, "Phased Arrays - Part II: Implementations, Applications, and Future Trends," *IEEE Transactions on Microwave Theory and Techniques*, Vol. 50, pp. 688–697, 2002.

[3] F. Capolino,M. Albani, S.Maci, and L. B. Felsen,"Frequency-domain green's function for a planar periodic semi-infinite phased array - part i: Truncated floquet wave formulation," *IEEE Transactions on Antennas and Propagation*, 48(1):67–74, January 2000.

[4] F. Capolino, M. Albani, S. Maci, and L. B. Felsen," Frequency-domain green's function for a planar periodic semi-infinite phased array - part ii: Diffracted wave phenomenology," *IEEE Transactions on Antennas and Propagation*, 48(1):75–85, January 2000.

[5] A. Polemi, A. Toccafondi, and S. Maci,"High-frequency green's function for a semiinfinite array of electric dipoles on a grounded slab - part i: Formulation," *IEEE Transactions on Antennas and Propagation*, 49(12):1667–1677, December 2001.

[6] A. Cucini, M. Albani, and S. Maci,"Truncated floquet wave full-wave analysis of large phased arrays of open-ended waveguides with a nonuniform amplitude excitation," *IEEE Transactions on Antennas and Propagation*, 51(6):1386–1394, June 2003.

[7] A. Cucini, M. Albani, and S. Maci,"Truncated floquet wave full-wave (t(fw)2) analysis of large periodic arrays of rectangular waveguides," *IEEE Transactions on Antennas and Propagation*, 51(6):1373–1385, June 2003.

[8] R.Mittra, C. H. Chan, and T. Cwik,"Techniques for analyzing frequency selective surfaces – a review," *IEEE Proceedings*, 76:1593–1614, December 1988.

[9] R. C. Hansen,"A gibbsianmodel for finite scanned arrays," *IEEE Transactions on Antennas and Propagation*, 44(2):243–248, February 1996.

[10] J. M. Usoff and B. A. Munk," Edge effects of truncated periodic surfaces of thin wire elements," *IEEE Transactions on Antennas and Propagation*, 42(7):946–953, July 1994.

[11] J. P. Skinner, C. C. Whaley, and T. K. Chattoraj," Scattering from finite-by-infinite arrays of slots in a thin conducting wedge," *IEEE Transactions on Antennas and Propagation*, 43(4):369–375, April 1995.

[12] C. Craeye, A. B. Smolders, D. H. Schaubert, and A. G. Tijhuis,"An efficient computation scheme for the free space green's function of a two-dimensional semiinfinite phased array," *IEEE Transactions on Antennas and Propagation*, 51(4):766–771, April 2003.

[13] A. J. Roscoe and R. A. Perrott, "Large finite array analysis using infinite array data," *IEEE Transactions on Antennas and Propagation*, volume 42, no. 7, pp. 983–992, (1994).

[14] A. K. Skrivervik and J. R. Mosig, "Finite phased array of microstrip patch antennas: The infinite array approach," *IEEE Transactions on Antennas and Propagation*, volume 40, no. 5, pp. 579–582, (1992).

[15] H. Holter and H. Steyskal, "On the size requirement for finite phased-array models," *IEEE Transactions on Antennas and Propagation*, volume 50, no. 6, pp. 836–840, (2002).

[16] A. K. Skrivervik and J. R. Mosig, "Analysis of finite phase arrays of microstrip patches," *IEEE Transactions on Antennas and Propagation*, volume 41, no. 8, pp. 1105–1114, (1993).

[17] B. Tomasic and A. Hessel, "Analysis of finite arrays - a new approach," *IEEE Transactions on Antennas and Propagation*, volume 47, no. 3, pp. 555–564, (1999).

[18] R.Mittra, C. H. Chan, and T. Cwik.,"Techniques for analyzing frequency selective surfaces – a review," *IEEE Proceedings*, Volume 76, no. 12, pp.1593–1614, (1988).

[19] R. W. Scharstein, "Mutual coupling in a slotted phased array, infinite in E-plane and finite in H-plane," *IEEE Transactions on Antennas and Propagation*, volume 38, no. 8, pp. 1186–1191, (1990).

[20] J. M. Usoff and B. A. Munk, "Edge effects of truncated periodic surfaces of thin wire elements," *IEEE Transactions on Antennas and Propagation*, volume 42, no. 7, pp. 946–953, (1994).

[21] C. Craeye, A. G. Tijhuis, and D. H. Schaubert, "An efficient mom formulation for finite by-infinite arrays of two-dimensional antennas arranged in a three-dimensional structure," *IEEE Transactions on Antennas and Propagation*, volume 52, no. 1, pp. 271–281, (2004).

[22] R. W. Kindt, K. Sertel, E. Topsakal, and J. L. Volakis, " Array decompostion method for the accurate analysis of finite arrays," *IEEE Transactions on Antennas and Propagation*, volume 51, no. 6, pp.1364–1372, (2003).

[23] L. Shafai and A.K. Bhattacharyya, "Input Impedance and Radiation Characteristics of Small Microstrip Phased Arrays Including Mutual Coupling MSAT Application," *ELectromagnetics*, volume 6, no. 4, pp. 333-349, (1986).

[24] A. A. Kishk, and S. L. Ramaraju, "Design of different configurations of finite microstrip arrays of circular patches," *International Journal of Microwave and Millimeter-Wave Computer Aided Engineering*, Vol. 4, No. 1, pp. 6-17, 1994.

[25] Ahmed A. Kishk**,"** Prediction of Large Array Chracteristics from Small Array Parameters," 2nd European Conference on Antennas and Propagation

(EuCAP 2007) Edinburgh, UK, 11-16 Nov. 2007, Page(s):p584-588.

[26]Shaya Karimkashi and Ahmad A. Kishk," Focusing Properties of Fresnel Zone Plate Lens Antennas in the Near-Field Region," *IEEE Transactions on Antennas and Propagations, Vol. 59, No. 5, pp* 1481 – 1487, May 2011.

[27]B. Kolundzija et. al. *WIPL-D Professional v5.1 Electromagnetic Modeling of Composite Metallic and Dielectric Structures: Software and Users Manual*, WIPL-D Ltd. 2004.

Biography of Dr. Ahmed A. Kishk

Ahmed A. Kishk is a Professor and Canada Reserch Chair in Advanced Antenna System at Concordia University, He is a distinguish lecturer for the Antennas and Propagation Society (2013-2015). He is now an Editor of Antennas & Propagation Magazine. He was an Editor-in-Chief of the ACES Journal from 1998 to 2001. He was the chair of Physics and Engineering division of the Mississippi Academy of Science (2001-2002). He is an AP AdCom member (2013-2015).

His research interest includes the areas of Dielectric resonator antennas, microstrip antennas, small antennas, microwave sensors, RFID antennas, Multi-function antennas, microwave circuits, EBG, artificial magnetic conductors, and phased array antennas. He has published over 240-refereed Journal articles and 380 conference papers. He is a coauthor of four books and several book chapters and editor of three books. He offered several short courses in international conferences.

Dr. Kishk received the 1995 and 2006 outstanding paper awards for papers published in the Applied Computational Electromagnetic Society Journal. He received the 1997 Outstanding Engineering Educator Award from Memphis section of the IEEE. He received the Outstanding Engineering Faculty Member of the Year on 1998 and 2009, Faculty research award for outstanding performance in research on 2001 and 2005. He received the Award of Distinguished Technical Communication for the entry of IEEE Antennas and Propagation Magazine, 2001. He also received The Valued Contribution Award for outstanding Invited Presentation, "EM Modeling of Surfaces with STOP or GO Characteristics – Artificial Magnetic Conductors and Soft and Hard Surfaces" from the Applied Computational Electromagnetic Society. He received the Microwave Theory and Techniques Society Microwave Prize 2004. He received 2013 Chen-To Tai Distinguished Educator Award of the IEEE Antennas and Propagation Society. In recognition "For contributions and continuous improvements to teaching and research to prepare students for future careers in antennas and microwave circuits, Dr. Kishk is a Fellow of IEEE since 1998, Fellow of Electromagnetic Academy, and Fellow of the Applied Computational Electromagnetic Society (ACES). He is a member of several Technical Societies.